Cardiology and Cardiovascular Research
2021; 5(3): 141-146
http://www.sciencepublishinggroup.com/j/ccr
doi: 10.11648/j.ccr.20210503.13
ISSN: 2578-8906 (Print); ISSN: 2578-8914 (Online)

Novel Animal Model for Ventricular Ejection Fraction Measured by MRI

Josefino Tunac[1, *], Frederick Valeriote[2], Joseph Media[2], Robert Knight[3]

[1]Arterez, Inc, White Lake, United States

[2]Departermet of Hematology-Oncology Research, Henry Ford Health System, Detroit, United States

[3]Departerment of Neurology-NMR Research, Henry Ford Hospital, Detroit, United States

Email address:

drjoe@arterez.com (J. Tunac)

[*]Corresponding author

To cite this article:

Josefino Tunac, Frederick Valeriote, Joseph Media, Robert Knight. Novel Animal Model for Ventricular Ejection Fraction Measured by MRI. *Cardiology and Cardiovascular Research.* Vol. 5, No. 3, 2021, pp. 141-146. doi: 10.11648/j.ccr.20210503.13

Received: August 18, 2021; **Accepted**: August 30, 2021; **Published**: September 11, 2021

Abstract: *Aim:* The objective of this study is to evaluate an animal model, herein called the Tunac Arterial Plaque (TAP) mouse as a model for reduced left ventricle ejection fraction (LVEF). Traditional mouse models involve genetically modified or surgically altered animals, whereas the TAP model is a wild mouse (C57Bl/6 strain) fed with a high fat diet and treated with an environmental chemical pollutant 3,3',4,4'-Tetrachlorobiphenyl (PCB) to mimic human lifestyle. Thus, the LVEF volume of treated and untreated mice will be measured per MRI, as well as an assessment for the presence of arterial plaque. *Methods and results:* Ten-week-old male C57/Bl6 mice were fed with either normal or high fat diet, acclimated for 1 week and then PCB was administered by gavage. Magnetic resonance imaging (MRI) was performed using a 7-Tesla Varian magnet. Briefly, the heart was aligned to the proper orientation, then an intragate scan was carried out for a CINE presentation (motion sensitive MRI in which a series of static images are obtained at various stages of the cardiac cycle and then played back as a movie). A black blood method was used that caused the blood to appear darker than the adjacent tissue and a CINE sequence to sort images, from which another program a (Medviso Segment) calculated percent ejection fraction (EF), heart rate (HR) and respiratory rate (RR). For the aorta and carotid artery imaging, cross-sectional images of the aortic arch were obtained, which produced multiple contrast weightings. Mice fed with normal diet showed normal ejection fraction volume (75.1%). The high fat diet alone without PCB also effectively reduced EF% (67.7%), and the lowest reduction in EF were for mice fed with high fat and PCB (57.2%). In the high fat-PCB-treated group, there was a gradual reduction in % EF starting at 2 weeks with 65.2% EF and 52.5% at the 8-wk time point. MRI scan of the aortal arch showed plaques in mice fed with high fat diet and PCB treatment. *Conclusions:* First to demonstrate LVEF per cine MRI in a wild non-surgical or non-genetically modified mouse model. Plaque formation in aortal arch was confirmed by MRI.

Keywords: Cardiac, Heart Failure, MRI, Ejection Fraction, Plaque, Mice

1. Introduction

1.1. Ejection Fraction (EF) and Heart Failure (HF)

An ejection fraction (EF) is the volume of blood ejected from the left ventricle with each heartbeat, which is used as a measure of the pumping efficiency of the heart. EF is calculated by dividing the volume of blood pumped by the volume collected at the end of diastolic filling.

HF (aka, CHF, or chronic heart failure) is a global pandemic affecting at least 26 million people worldwide and is increasing in prevalence [1] affecting approximately 1 - 2% of adult population. HF accounts for more than 80,000 deaths annually in the US and an estimated $69.8 billion in annual health care spending by 2030 [2]. Based on left ventricular (LV) ejection fraction (LVEF), HF can be categorized in two types: reduced ejection fraction (HFrEF; LVEF < 40%), and preserved ejection fraction (HFpEF; LVEF ≥50%). HFrEF takes place when the heart muscles fail to squeeze properly to pump an adequate

amount of oxygen-rich blood to other parts of the body during systolic phase, while HFpEF takes place when the left ventricle fails to fill properly during diastolic phase [3]. Of the estimated 5 million patients in the US diagnosed with HF, approximately 50% are HFpEF and its prevalence is increasing by about 1% annually [4], relative to that of HFrEF incidence [5]. In between is a novel category recently introduced by the European Society of Cardiology (ESC) Guidelines on Acute and Chronic Heart Failure, called heart failure with mid-range ejection fraction (HFmrEF; LVEF 40–49%) [6, 7]. The percentage of the HF population that falls into the HFmrEF category is 13 - 24%, which is approximately 1.6 million individuals in the United States [8].

There are no effective treatments for HFpEF largely because of its pathophysiological heterogeneity [9]. In contrast drug treatments are available for HfrEF, e.g., triple therapy with ACEi/ARB, B blocker and MRA, ARNI (Sacubitril/Valsartan) Ivabradine/nitrates/digoxin [10-12]. *A* typical animal model for HfpEF involves a genetically modified mouse lacking osteopontin, treated with aldosterone and 1% sodium chloride (NaCl) to induce blood pressure elevation, cardiac hypertrophy, and fibrosis [13-15].

Recently, a noninvasive and nongenetically modified model of HFpEF was reported, which involved treating the mice with combination of high fat diet (HFD) and N [w]-nitro-l-arginine methyl ester (L-NAME) to inhibit nitric oxide (NO) synthase. The rationale is that the X-box binding protein 1 (Xbp1s) was found reduced in the myocardium of HfpEF patients due to increase NO synthase (iNOS) activity [16].

HF is a multifactorial, systemic disease triggered by damaged heart muscle (myocardium), followed by the activation of structural, neurohumoral, cellular, and molecular mechanisms to maintain physiological functioning [17]. Our paradigm is that the disruption of the endothelial glycocalyx is the upstream component of HF, which triggers coronary plaques and contributes to myocyte stiffness and reduced EF volume particularly in the left ventricle [18]. Meanwhile, MI is the most visible symptom, which develops HF and a sequalae of downstream diseases including, decreased renal function and sympathetic nervous system (SNS) and activation of the renin–angiotensin–aldosterone system (RAAS), Neurohumoral factors, such as SNS, RAAS, and arginine vasopressin (AVP), are biological defense mechanisms that preserve arterial volume and circulatory homeostasis during acute systemic volume depletion and low cardiac output, which is the endpoint of HF (Figure 1).

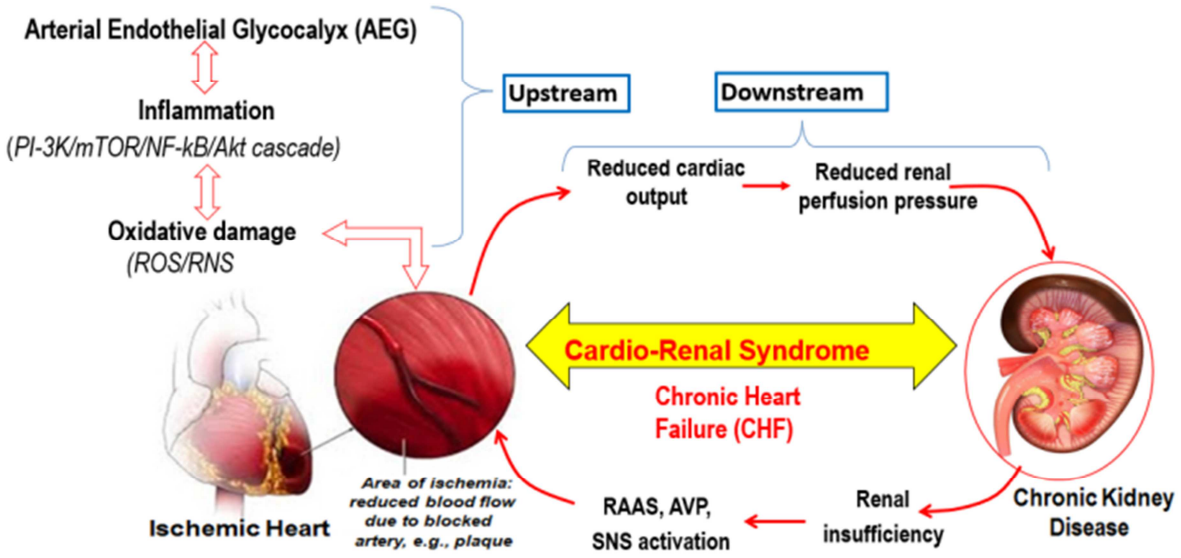

Figure 1. *Disrruption of the arterial endothelial glycocalyx triggers a cascade of diseases including the cardio-renal syndrome and chronic heart failure (CHF).*

1.2. Cardiac Magnetic Resonance Imaging (MRI) for EF

EF can be determined using several invasive and non-invasive imaging modalities, either subjectively by visual estimation or objectively by quantitative methods [i.e., echocardiography, magnetic resonance imaging (MRI), computed tomography (CT), gated equilibrium radionuclide angiography (commonly referred to as multiple-gated acquisition [MUGA] scan) and gated myocardial perfusion imaging with either single-photon emission computed tomography (SPECT) or positron emission tomography (PET)]. In the clinical setting, cardiac MRI and blood pool SPECT are considered as gold standards for the assessment of LVEF [19], but have not found wide use for monitoring cardiac therapies in mice.

One of the early high-resolution MRI sequences for assessment of myocardial function and morphology in mice describes a cine performed with prospective ECG gating using a spoiled gradient echo technique and quantitative analysis using a semi-automated approach [20]. Indeed, MRI has been used for calculation of EF function in both healthy and MI-induced mice [21]. In mice with permanent ischemic cardiomyopathy (ICM) or transient LAD ligation [22] and in different mouse models of cardiovascular diseases [23].

2. Materials and Methods

2.1. Mice

Ten ten-week-old male C57/Bl6 mice were obtained from Jackson Laboratories. Either normal or high fat (60% fat) diet (D12451, DIO series diet, Opensource Diets) were assigned per experiment group below upon receipt. Animals were acclimated for 1 week and then PCB was administered by gavage according to the following schedule.

Group 1 (mice 1,2) – regular chow diet (Control group);

Group 2 (mice 3-8) – high fat diet + PCB (2X per week for 2 weeks);

Group 5 (mice 9,10) – high fat diet only.

2.2. Treatments

3,3',4,4'-Tetrachlorobiphenyl (PCB-77) was obtained from Neosyn Laboratories. The dry chemical was suspended in 15.22 ml of corn oil to deliver 200 µmol/kg in 0.2 ml by gavage per mouse according to the treatment schedule. All experiments were approved by the Institutional Animal Care and Use Committee. All reagents were acquired from Sigma-Aldrich (St. Louis, MO) unless otherwise stated.

2.3. Magnetic Resonance Imaging (MRI)

All studies were performed using a 7-Tesla Varian magnet interfaced to a Bruker console running Paravision 6.0. Briefly, the heart was aligned to the proper orientation, then an intragate scan was carried out for a CINE presentation (a motion sensitive MRI in which a series of static images are obtained at various stages of the cardiac cycle and then played back as a movie). A black blood method, which caused the blood to appear darker than the adjacent tissue, was used. The CINE sequence required approximately 10 minutes and acquired a large set of images that were then sorted and reordered by the software. Afterwards, another program (Medviso Segment), was used to auto detect end diastole/end systole and calculate percent ejection fraction (EF), heart rate (HR) and respiratory rate (RR).

All studies were performed using a 7-Tesla Varian magnet (Figure 2) interfaced to a Bruker console running Paravision 6.0. Briefly, the heart was aligned to the proper orientation, then an intragate scan was carried out for a CINE presentation (motion sensitive MRI in which a series of static images are obtained at various stages of the cardiac cycle and then played back as a movie). We used a black blood method that causes the blood to appear darker than the adjacent tissue). The CINE sequence required approximately 10 minutes and acquired hundreds of images that were then sorted and reordered by the software. Afterwards, another program (Medviso Segment), was used to auto detect end diastole/end systole and calculate percent ejection fraction (EF), heart rate (HR) and respiratory rate (RR).

All animals received a baseline MRI scan including a 3-plane localizer scan that was used to position the animal within the magnet. This sequence was then followed by an intragate scan procedure (Bruker Corporation) which produced a series of images that were used to align the heart to the proper orientation to estimate EF using CINE imaging. A CINE is a special type of MRI data set in which a series of static images are obtained at different times (i.e., different stages of the cardiac cycle) and then played back as a movie. This technique is useful for evaluating tissues that move such as the heart, flowing blood, or cerebral spinal fluid. It is also occasionally used in evaluating bowel, joint or muscle motion. As noted, the resulting images were used to estimate the EF. The MRI scan technique used is referred to as a black blood method that caused the blood to appear darker than the adjacent tissue. The complete gradient-echo MRI intragate sequence (TR=20 ms, TE=2.6 ms, FOV=25 mm, 256x256 matrix size, single slice, 1 mm slice thickness) required approximately 10 minutes and produced a set of images that were later sorted and reordered by the software. As previously noted, the protocol used for the EF imaging produced a set of images showing the heart at various stages of the cardiac cycle that could be displayed as movie. The resulting data were used to estimate EF, HR, and RR.

For the aorta & carotid artery imaging, we devised a method for obtaining cross-sectional images of the aortic arch. The method produced multiple contrast weightings using a gradient-echo sequence (TR=30 ms, TE=4.2 ms, FOV=25 mm, 256x256, 5 slices 0.5 mm thick). To cover majority of the arch, the 5-slice data set was run three times at three different angles to cover the ascending, plateau, and descending sections of the aorta. The cross-sectional images were reviewed for the presence of suspected plaques by two senior scientists (JT and RK), however, the results were not verified histologically.

Additional contrast enhanced scans were performed in some animals after the CINE and aorta imaging. Once the data were collected, they were transferred offline for processing. To estimate the ejection fraction, we used a program called Medviso Segment. After opening the data set and displaying the images in Segment, we used a command to auto detect end diastole and end systole. This provided the EF data as a %. All animal groups were studied at multiple time points after treatment except for the two that received the HFD only.

3. Results

3.1. General Mouse Health

No mice died during the study, and no adverse effects were noted due to administration of PCB. No notable gross changes in weight, respiratory or heart rates attributable to the diet and PCB.

3.2. Ejection Fraction Among Treatments

Mice fed with normal diet showed normal ejection fraction volume (75.1%). The high fat diet alone without PCB also effectively reduced EF% (67.7%), and the lowest reduction in EF were for mice fed with high fat and PCB (57.2%), Figure 2.

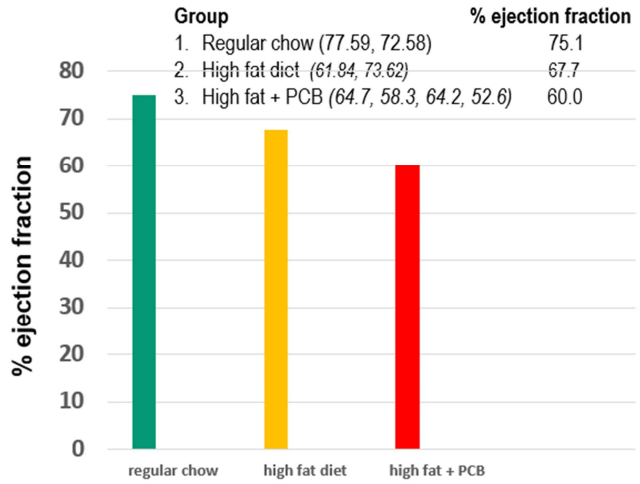

Figure 2. *Ejection fraction profile in Tap mouse was most reduced when treated with high fat diet and PCB Progression in reduction of ejection fraction (EF) volume.*

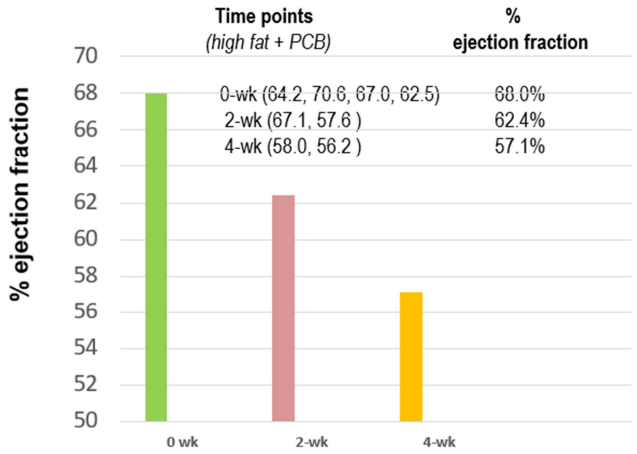

Figure 3. *Progressive reduction in ejection volume from in the Tap mouse treated with high fat diet and PCB MRI imaging of aortal arch.*

Focusing on the high fat-PCB-treated group, there was a gradual reduction in % EF starting at 2 weeks with 65.2% EF and 52.5% at the 8-wk time point (Figure 3).

Due to their small dimensions and nearly constant motion, MR imaging of coronary arteries for plaques is virtually impossible in mouse. Thus, e next option was an MRI scan of the aortal arch was carried out, which were found in mice fed with high fat diet and PCB treatment (Figure 4).

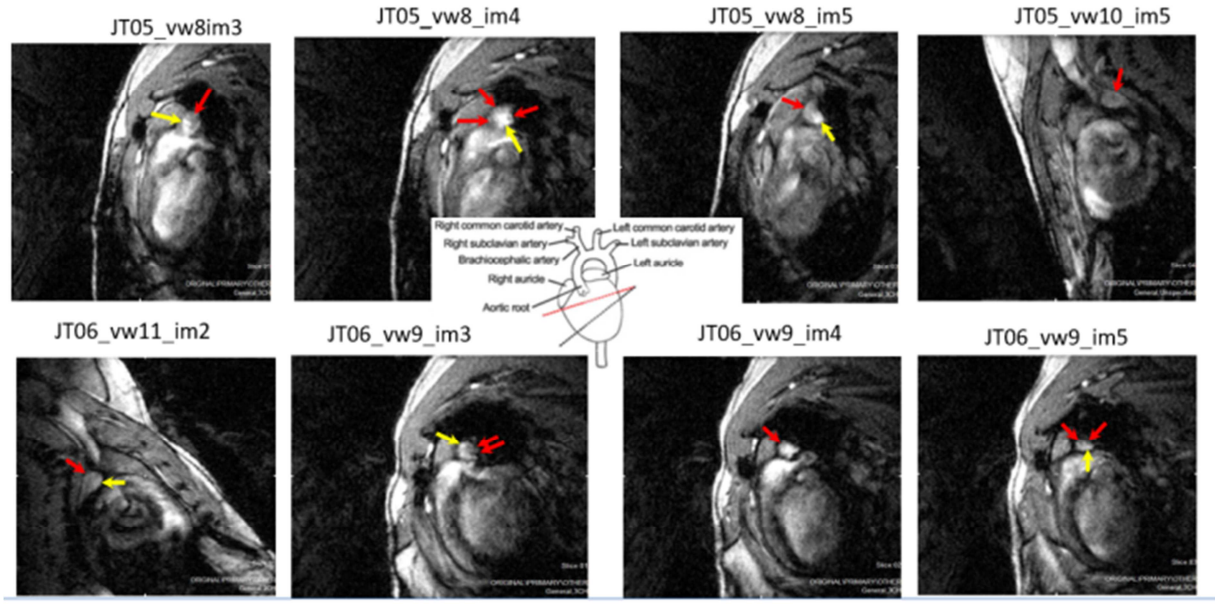

Figure 4. *MRI scans of mice (05 & 06) showing suspected areas of plaques in the aortal arch (red and yellow arrows).*

4. Discussion

Man-made chemical pollutants are part of the equation that triggers multifactorial diseases. The complex etiology of diseases is of multiple (plexic) origin, and disease manifestations are equally complex, herein called xenoplexic diseases including the family of CVD, inflammatory, neurological, immunological, hematological, endocrine disorders, cancer, macular dysfunction, etc. Pollutants are found in foods, beverages and packaging, clothes, cosmetics and cleaning products, furniture, paints, electronic equipment, plastics, and the list is long. Persistent pollutants including the lipophilic persistent organic pollutants (POPs) polychlorobiphenyls (PCBs) bio-accumulate in fatty tissues [24]. PCB was chosen for this study because they are the most ubiquitous environmental pollutant. PCBs are resistant to acids and bases as well as to heat and have been used as an insulating material in electric equipment, such as transformers and capacitors, and in heat transfer fluids and in lubricants, as plasticizers, surface coatings, inks, adhesives, flame-retardants, paints, and carbonless duplicating paper. Since 1929 around 2 million ton of PCBs have been produced, about 10% of which remain in the environment today [25]. Pollutants disrupt certain signaling and differentiation pathways and induce inflammation in the adipose tissue [26]. Pollutants and

other blood debris trapped in a stagnant blood flow, due to high level of fat packaging lipoprotein (VLDL), triggers inflammation, disruption of AEG, plaque formation and cardiovascular diseases (Figure 5).

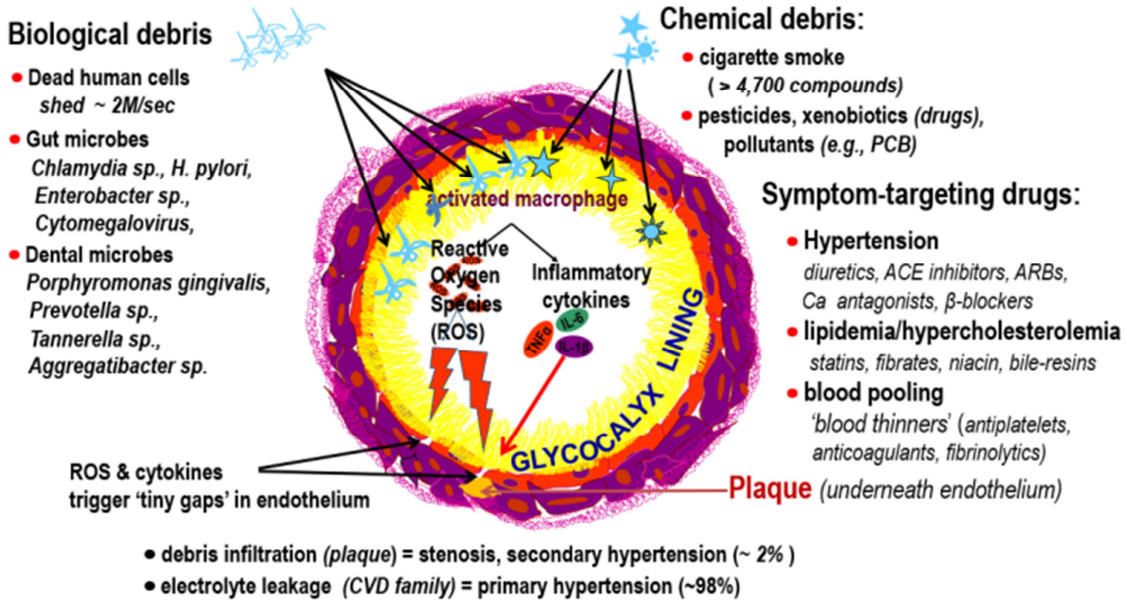

Figure 5. *Biological and chemical pollutants in the arterial bends triggers inflammation, tiny endothelial gaps creating electrolyte leakage (hypertension) and debris infiltration (plaque).*

Plaques stiffen myocytes or trigger apoptosis, disrupt pumping and reduced LVEF [27]. While MRI has become a routine imaging to assess the myocardium in the clinic, coronary artery imaging offers challenges because of both their small caliber and complex motion. In animal models, MRI has been used to detect plaques in aortal arch [28]. Because, of the impossibility of scanning plaques in the coronaries of mice, detection of plaques in the aorta infers plaque formation in the coronaries. Moreover, our previous study where mice with high fat diet and PCB [18] showed well-formed plaque formation in the brachiocephalic artery.

5. Conclusion

In summary, this study demonstrates plaque formation in the aortal arch, which is good indication of plaque formation in the coronary arteries. Thus, the TAP mouse may well be a promising model for evaluating HF drugs vs. HF.

Conflict of Interest

The authors declare no competing interests.

References

[1] Ponikowski P, Anker S, AlHabib K, Cowie M, Force T, Hu S, et al. (2014). Heart failure: Preventing disease and death worldwide ESC Heart Fail, 1: 4-25.

[2] Virani S, Alonso A, Benjamin E, Marcio S, Bittencourt M, Callaway C, et al. (2020). Heart disease and stroke statistics—2020 update: A report from the american heart association. Circulation, 141: e139-e596.

[3] Borlaug B. (2014). The pathophysiology of heart failure with preserved ejection fraction. Nat. Rev. Cardiol, 11: 507-515.

[4] Pfeffer M, Shah A, Borlaug B. (2018). Heart failure with preserved ejection fraction in perspective. Circ Res, 124: 1598-1617.

[5] Shah S, Kitzman D, Borlaug B, van Heerebeek L, Zile M, Kass D, et al. (2016). Phenotype-specific treatment of heart failure with preserved ejection fraction. Circulation, 134: 73-90.

[6] Oeing C, Tschöpe C, Pieske B. (2016). The new ESC guidelines for acute and chronic heart failure 2016. Herz, 41: 655-663.

[7] Ponikowski P, Voors A, Anker S, Bueno H, Cleland J, Coats A, et al. (2016). 2016 ESC guidelines for the diagnosis and treatment of acute and chronic heart failure: The task force for the diagnosis and treatment of acute and chronic heart failure of the european society of cardiology (ESC). Eur Heart J, 37: 2129–2200.

[8] Hsu J, Ziaeian B, Fonarow G. (2017). Heart failure with mid-range (borderline) ejection fraction: Clinical implications and future directions. JACC Heart Fail, 5: 763-771.

[9] Tibrewala A, Yancy C. (2019). Heart failure with preserved ejection fraction in women. Heart Fail Clin, 15: 9-18.

[10] Deng Y, Xie M, Li Q, Xu X, Ou W, Zhang Y, et al. (2021). Targeting mitochondria-inflammation circuit by β-hydroxybutyrate mitigates HFpEF. Circ Res, 128: 232-245.

[11] Roh J, Houstis N, Rosenzweig A. (2017). Why don't we have proven treatments for HFpEF? Circ Res, 120: 1243-1245.

[12] Yoon S, Eom G. (2019). Heart failure with preserved ejection fraction: Present status and future directions. Exp Mol Med, 51: 1-9.

[13] Sam F, Xie Z, Ooi H, Kerstetter D, Colucci W, Singh M, et al. (2004). Mice lacking osteopontin exhibit increased left ventricular dilation and reduced fibrosis after aldosterone infusion. Am J Hypertens, 17: 188-193.

[14] Tsukamoto Y, Mano T, Sakata Y, Ohtani T, Takeda Y, Tamaki S, et al. (2013). A novel heart failure mice model of hypertensive heart disease by angiotensin ii infusion, nephrectomy, and salt loading. Am J Physiol Heart Circ Physiol, 305: H1658-1667.

[15] Valero-Muñoz M, Backman W, Sam F. (2017). Murine models of heart failure with preserved ejection fraction: A "fishing expedition". JACC Basic Transl Sci, 2: 770-789.

[16] Schiattarella G, Altamirano F, Tong D, French K, Villalobos E, Kim S, et al. (2019). Nitrosative stress drives heart failure with preserved ejection fraction. Nature, 568: 351-356.

[17] Lüscher T. (2016). Heart failure and left ventricular remodelling in HFrEF and HFpEF. Eur Heart J, 37: 423-424.

[18] Wooley P, Tunac J. (2017). A novel model of atherosclerosis in mice J Clin Exp Cardiolog, 8: 1.

[19] Xie B, Tian Y, Zhang J, Zhao S, Yang M, Guo F, et al. (2012). Evaluation of left and right ventricular ejection fraction and volumes from gated blood-pool SPECT in patients with dilated cardiomyopathy: Comparison with cardiac MRI. J Nucl Med, 53: 584-591.

[20] Higuchi T, Nekolla S, Jankaukas A, Weber A, Huisman M, Reder S, et al. (2007). Characterization of normal and infarcted rat myocardium using a combination of small-animal PET and clinical MRI. J Nucl Med, 48: 288-294.

[21] Kreissl M, Wu H, Stout D, Ladno W, Schindler T, Zhang X, et al. (2006). Noninvasive measurement of cardiovascular function in mice with high-temporal-resolution small-animal PET. J Nucl Med, 47: 974-980.

[22] Stegger L, Heijman E, Schafers K, Nicolay K, Schafers M, Strijkers G. (2009). Quantification of left ventricular volumes and ejection fraction in mice using PET, compared with MRI. J Nucl Med, 50: 132-138.

[23] Brunner S, Todica A, Böning G, Nekolla S, Wildgruber M, Lehner S, et al. (2012). Left ventricular functional assessment in murine models of ischemic and dilated cardiomyopathy using [18 f] fdg-PET: Comparison with cardiac MRI and monitoring erythropoietin therapy. EJNMMI Res, 2: 43.

[24] O'Grady Milbrath M, Wenger Y, Chang C, Emond C, Garabrant D, Gillespie B, et al. (2009). Apparent half-lives of dioxins, furans, and polychlorinated biphenyls as a function of age, body fat, smoking status, and breast-feeding. Environ Health Perspect, 117: 417-425.

[25] Faroon O, Ruiz P. (2016). Polychlorinated biphenyls: New evidence from the last decade. Toxicol Ind Health, 32: 1825-1847.

[26] Hue O, Marcotte J, Berrigan F, Simoneau M, Doré J, Marceau P, et al. (2007) Plasma concentration of organochlorine compounds is associated with age and not obesity. Chemosphere, 67: 1463-1467.

[27] van Empel V, Bertrand A, Hofstra L, Crijns H, Doevendans P, De Windt L. (2005). Myocyte apoptosis in heart failure. Cardiovasc Res, 67: 21-29.

[28] Trogan E, Fayad Z, Itskovich V, Aguinaldo J, Mani V, Fallon J, et al. (2004). Serial studies of mouse atherosclerosis by in vivo magnetic resonance imaging detect lesion regression after correction of dyslipidemia. Arterioscler Thromb Vasc Biol, 24: 1714-1719.